J. Phys. B: At. Mol. Phys. **14** (1981) 2921–2934. Printed in Great Britain

Total cross sections for electron excitation transitions between the 1^1S, 2^3S, 2^1S, 2^3P and 2^1P states of atomic helium

W C Fon†, K A Berrington, P G Burke‡ and A E Kingston

Department of Applied Mathematics and Theoretical Physics, The Queen's University of Belfast, Belfast, BT7 1NN, Northern Ireland

Received 16 January 1981, in final form 27 March 1981

Abstract. The five-state R-matrix calculations of Berrington and co-workers on the excitation of helium by electrons have been revised and extended to higher electron impact energies. Inelastic scattering cross sections are presented for all transitions between the 1^1S, 2^3S, 2^1S, 2^3P and 2^1P states of helium, and elastic cross sections are presented for the $n = 2$ states.

1. Introduction

In the study of laboratory plasmas it is important to have an accurate knowledge of cross sections for excitation of atoms and ions by electron collisions. Helium is of particular interest since it is used for example in gas discharge plasma, in rare-gas lasers (Flannery *et al* 1975) and in fusion research plasmas. It is also important in astrophysical plasmas (Tully and Summers 1979). It is desirable, therefore, to obtain accurate cross sections for electron collision processes in helium.

While considerable theoretical and experimental effort has been devoted to obtaining cross sections for the scattering of low-energy electrons from ground-state helium (see Fon *et al* 1979, 1980), relatively little is known about collisions between electrons and the $n = 2$ levels of helium. The present calculation represents the first *ab initio* theoretical estimates of these cross sections over a wide range of electron impact energies.

At low energies, Burke *et al* (1969) have carried out a close-coupling calculation on the transitions between $n = 1$ and $n = 2$ states of helium. Because of the complexity of the close-coupling equation and the relatively small computing power available at that time they were forced to make simplifications about the contribution from the exchange terms. These simplifications may give rise to inaccurate results. Oberoi and Nesbet (1973) have solved the Bethe–Goldstone continuum equation variationally in the energy range between the $n = 2$ and $n = 3$ thresholds. Berrington *et al* (1975) have carried out five-state R-matrix calculations over a similar energy range. Both of these elaborate calculations only give transitions over a small energy range and the number of

† Commonwealth Fellow on sabbatical leave from the Department of Mathematics, University of Malaya, Kuala Lumpur, Malaysia.

‡ Also at: Science Research Council, Daresbury Laboratory, Daresbury, Warrington, WA4 4AD, England.

0022-3700/81/162921+14$01.50

partial waves that they were able to include in these calculations was not sufficient to ensure convergence, in particular for transitions between optically allowed transitions. It seems also that these calculations have not included all the possible parities (even and odd parities for transitions from P to P target states). While the lack of convergence, due to the inclusion of an insufficient number of partial waves, seriously underestimates the cross sections at the upper end of their energy range, certain parity contributions substantially underestimate the P–P cross sections at low energies. However, for other transitions at low energies the present results agree with the earlier calculations of Berrington *et al* (1975).

Apart from these two elaborate calculations, other calculations for transitions between the $n = 2$ states are: first Born approximation (Bhattacharyya 1961, Taylor 1975, Moiseiwitsch 1957, Kennedy 1968, Ton-That *et al* 1977, Flannery *et al* 1975), Glauber approximation (Chen and Khayrallah 1976), close-coupling approximation (Marriott 1966), effective potential calculation (Robinson 1969), polarised-core approximation (Husain *et al* 1967), extended-polarisation approximation (Sklarew and Callaway 1968) and ten-channel eikonal calculations (Flannery and McCann 1975). Among these, large discrepancies in magnitude, as well as in shape, still exist. None gives a full account of all transitions between $n \leqslant 2$ states over a wide energy range.

2. *R*-matrix calculation

In this paper we extend the earlier calculation of Berrington *et al* (1975) on the excitation of helium to energies up to about 200 eV for all transitions between $n = 1$ and 2 states. We adopt the same R-matrix boundary radius $a = 16.044$ au, but we include 25 continuum orbitals instead of 20 for each angular momentum. The calculation is carried out retaining the first five atomic eigenstates (1^1S, 2^3S, 2^1S, 2^3P, 2^1P) which are represented by the same CI wavefunctions as in the earlier calculation.

In this paper, no attempt has been made to overcome the difficulty in our calculation arising from the pseudo-resonances which occur in the energy range $30 \leqslant E \leqslant 80$ eV (see Fon *et al* 1979, 1980). Although work is well underway to tackle the problem of pseudo-resonances for excitation from the ground state, this does not unduly limit the usefulness of the present calculation for transitions between $n = 2$ states. In comparison with excitations from the ground state, the threshold energies of the $n = 2$ states lie very close to each other. Because of the narrow energy spacing between $n = 2$ states, electron scattering from $n = 2$ metastable states with impact energy 10 eV (above the $n = 2$ thresholds) already enters well inside the intermediate energy range where a less elaborate method like the eikonal or the Glauber approximations may be valid. In particular the spin-forbidden transitions between $n = 2$ states are significant only for $E < 10$ eV above $n = 2$ thresholds where the present R-matrix calculation is free of pseudo-resonances and is expected to be good. For spin-allowed transitions between $n = 2$ states, the shape of cross sections as functions of energy has already been established by energy points less than 10 eV above $n = 2$ thresholds. In this paper we extrapolate the cross section from below 10 eV to join up with energy points greater than 60 eV (above $n = 2$ thresholds) where cross sections can be calculated without the complication of pseudo-resonances.

For the optical, spin-allowed transitions between $n = 2$ states $2^3S \rightarrow 2^3P$ and $2^1S \rightarrow 2^1P$, large numbers of partial waves contribute to the calculation of integrated cross

sections. This is due to the long-range dipole character of the interaction resulting from the coupling between the close-lying S state ($2^{1,3}S$) and P state ($2^{1,3}P$). For all the results presented in this paper T-matrix elements for partial waves up to $L = 13$ are obtained from the R-matrix program. For $L \geqslant 14$, the T-matrix elements are obtained by a five-state unitarised Born approximation using the same CI wavefunctions as in the R-matrix program. Since the convergence of the partial-wave series for the total cross section is slowest for the $2^3S \rightarrow 2^3P$ and $2^1S \rightarrow 2^1P$ transitions, the number of partial waves used at a given energy is determined by these transitions.

In practice the cross section was calculated with a certain number of partial waves and the contribution from higher partial waves was estimated by assuming that the contributions from the higher partial waves formed a geometric series. The number of partial waves was then increased by about 20 and a new estimate of the cross section was obtained. This was repeated until the two results agreed to within about 0.1%. As a final check on our optically allowed cross section we compared the leading term in the high-energy expansion of the cross section, $A \lg E/E$, with A obtained directly from the theoretical oscillator strength (i.e. $A = 60.9 f/\Delta E$); there was excellent agreement between the two results. For $k_1^2 = 7.3169$ we used 150 partial waves but for $k_1^2 = 2.14$ we only required 80 partial waves.

For elastic scattering from the 2^3S and 2^1S states, T-matrix elements for higher ($L > 14$) partial waves are calculated using the formula (Rosenberg *et al* 1961)

$$\tan \delta_L = \frac{\pi \alpha k^2}{(2L+3)(2L+1)(2L-1)} \tag{1}$$

where α is the respective dipole polarisability of the 2^3S and 2^1S states.

As explained in the calculation of Berrington *et al* (1975), the calculated energy differences between the $n = 2$ states are in good agreement with experiment; however, the calculated energy of the ground state is too high in comparison with experiment. As a result, the calculated value of $E(2^3S) - E(1^1S) = 0.7105$ au instead of the observed value of 0.7285 au. In presenting our results, the incident electron energy is given as energy above respective thresholds in all our figures and tables, so no renormalisation is required.

3. Results and discussion

We have calculated the integrated cross sections for the transitions between the five lowest states of helium (1^1S, 2^3S. 2^1S, 2^3P and 2^1P), and results are given in tables 1–4. The present calculations are also shown in figures 1–8 and compared with other theoretical calculations and experimental measurements whenever possible.

Results are not presented for the elastic scattering of the ground state, 1^1S, of helium. These results are not expected to be accurate with the current choice of target functions as the 1^1S–2^1P coupling only provides about 70% of the long-range dipole polarisation potential which is important for low-energy elastic scattering. Accurate cross sections for the elastic scattering by the ground state have recently been presented (O'Malley *et al* 1979) at low electron energies and by Fon *et al* (1981) for higher energies. These calculations include pseudo-states which give the long-range dipole polarisation potential almost exactly.

3.1. The n = 1 to n = 2 excitation cross sections

The cross sections for these transitions are given in tables 1, 2, 3 and 4. As similar results have already been reported and discussed in full in previous papers (Fon *et al* 1979, 1980) we shall not consider them here.

3.2. The n = 2 to n = 2 cross sections

3.2.1. Cross sections for spin-forbidden transitions: $2^3S \rightarrow 2^1S$, $2^3S \rightarrow 2^1P$, $2^1S \rightarrow 2^3P$ and $2^3P \rightarrow 2^1P$. In contrast to spin-allowed and optically allowed transitions, cross sections for spin-forbidden transitions are dominated by short-range exchange potentials and hence we may expect only a few low-lying partial waves to contribute to the calculation of integrated cross sections. For energies of 10 eV or less (above the $n = 2$ thresholds), it is sufficient to include partial waves up to $L = 13$. However, at energies of 60 eV or more (above the $n = 2$ thresholds) the situation is more complex. It is found that for S–S or P–P transitions it is still sufficient to include only partial waves up to $L = 13$ but for S–P transitions higher partial waves contribute significantly and our results are therefore not reliable for $E > 10$ eV above threshold.

The integrated cross sections for these spin-forbidden transitions are given in tables 1, 2, 3 and 4 and are shown in figures 1 and 2. No experimental measurements are available for comparison. The only calculations which have been carried out are those

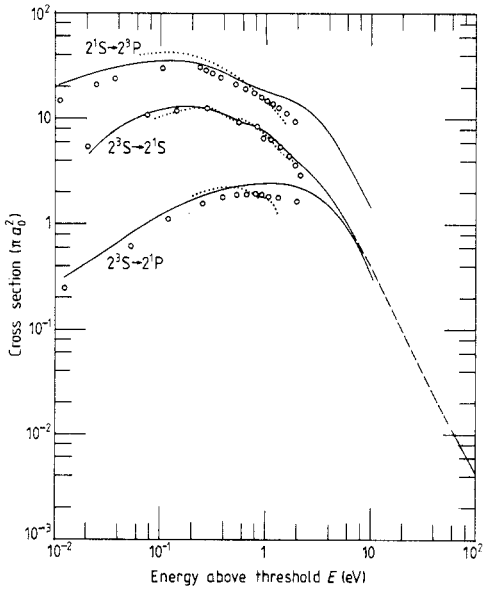

Figure 1. Cross sections (in units of πa_0^2) for the spin-forbidden transitions: $e + He^*(2^3S) \rightarrow e + He^*(2^1P)$, $e + He^*(2^3S) \rightarrow e + He^*(2^1S)$ and $e + He^*(2^1S) \rightarrow e + He^*(2^3P)$ against electron impact energy (in eV) above 2^1P, 2^1S and 2^3P thresholds respectively. Theoretical results: ———, present R-matrix five-state calculation; – – –, interpolation of present R-matrix five-state calculation (see § 4); · · · ·, Oberoi and Nesbet (1973); ∘ ∘ ∘, R-matrix five-state calculation (Berrington *et al* 1975).

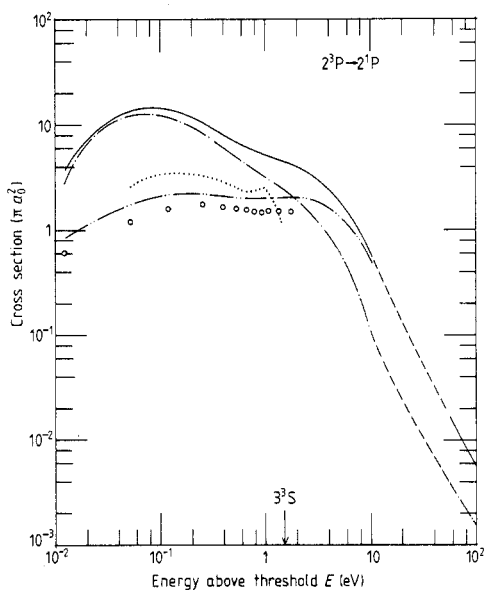

Figure 2. Cross sections (in units of πa_0^2) for $2^3P \rightarrow 2^1P$ spin-forbidden transition: data legend as figure 1 with —··—, present R-matrix calculation with even parity; —·—, present R-matrix calculation with odd parity; – – –, interpolation of present R-matrix calculation (see § 4).

Table 1. Electron excitation cross section (πa_0^2) for the $1^1S \rightarrow 2^3S$ and $2^3S \rightarrow 2^3S$ transitions.

E (eV) above 2^3S threshold	$1^1S \rightarrow 2^3S$	$2^3S \rightarrow 2^3S$	E (eV) above 2^3S threshold	$1^1S \rightarrow 2^3S$	$2^3S \rightarrow 2^3S$
0.0128	9.959^{-3}†	1.551^{2}	1.413	4.807^{-2}	2.134^{2}
0.0264	1.327^{-2}	1.225^{2}	1.482	4.689^{-2}	2.056^{2}
0.0400	1.602^{-2}	1.439^{2}	1.618	4.557^{-2}	1.936^{2}
0.0536	1.870^{-2}	1.767^{2}	1.754	4.499^{-2}	1.840^{2}
0.122	3.375^{-2}	3.222^{2}	1.890	4.468^{-2}	1.745^{2}
0.258	6.200^{-2}	4.099^{2}	2.026	4.455^{-2}	1.656^{2}
0.394	6.952^{-2}	3.685^{2}	2.162	4.460^{-2}	1.568^{2}
0.530	6.398^{-2}	3.141^{2}	2.298	4.476^{-2}	1.482^{2}
0.666	5.436^{-2}	2.730^{2}	2.434	4.501^{-2}	1.399^{2}
0.734	4.783^{-2}	2.583^{2}	2.706	4.576^{-2}	1.247^{2}
0.774	4.191^{-2}	2.515^{2}	2.978	4.680^{-2}	1.119^{2}
0.788	3.791^{-2}	2.500^{2}	3.250	4.805^{-2}	1.013^{2}
0.802	3.664^{-2}	2.464^{2}	3.522	4.941^{-2}	9.258^{1}
0.815	3.598^{-2}	2.470^{2}	3.794	5.079^{-2}	8.523^{1}
0.870	3.819^{-2}	2.533^{2}	4.474	5.394^{-2}	7.104^{1}
0.937	4.411^{-2}	2.622^{2}	5.154	5.632^{-2}	6.073^{1}
1.073	5.525^{-2}	2.719^{2}	6.514	5.868^{-2}	4.636^{1}
1.087	5.591^{-2}	2.737^{2}	6.684	5.872^{-2}	4.500^{1}
1.100	5.621^{-2}	2.777^{2}	7.874	5.699^{-2}	3.711^{1}
1.114	5.637^{-2}	2.769^{2}	9.784	4.779^{-2}	2.945^{1}
1.127	5.657^{-2}	2.732^{2}	1.0594^{1}	4.281^{-2}	2.692^{1}
1.195	5.656^{-2}	2.694^{2}	6.1814^{1}	—	5.658
1.209	5.486^{-2}	2.509^{2}	8.0184^{1}	2.300^{-3}	4.474
1.345	5.007^{-2}	2.236^{2}	1.00184^{2}	1.392^{-3}	3.657
1.372	4.901^{-2}	2.192^{2}	1.30184^{2}	7.840^{-4}	2.873
			1.80184^{2}	3.611^{-4}	—

† The superscript denotes the power of ten by which the number should be multiplied.

of Oberoi and Nesbet (1973), Burke *et al* (1969) and Berrington *et al* (1975). The present calculations agree very well with those of Oberoi and Nesbet (1973) for all the spin-forbidden transitions expect that of $2^3P \rightarrow 2^1P$. For a P-state–P-state transition both even and odd parity contribute to the scattering cross sections. The odd additional parity contributions were certainly omitted by Berrington *et al* (1975) and may have been omitted by Oberoi and Nesbet (1973). These two calculations substantially underestimate the scattering cross section at low energies (see figure 2).

3.2.2. Cross sections for optically allowed transitions: $2^3S \rightarrow 2^3P$ and $2^1S \rightarrow 2^1P$. The $2^3S \rightarrow 2^3P$ and $2^1S \rightarrow 2^1P$ transitions have important applications in plasma diagnostics and in astrophysics. Unfortunately, current information on these transitions is very limited.

Burke *et al* (1969) reported some preliminary results obtained using the close-coupling approximation. It is not clear to what extent the approximation discussed in § 1 would affect the reliability of their results for $2^{1,3}S \rightarrow 2^{1,3}P$ transitions. Oberoi and Nesbet (1973) and Berrington *et al* (1975) have also carried out calculations for these transitions; however, only a few partial waves were taken into consideration in their calculations. These calculations are therefore not expected to be good since the contribution from high partial waves is particularly dominant for these transitions.

Table 2. Electron excitation cross section (πa_0^2) for the $1^1S \rightarrow 2^1S$, $2^3S \rightarrow 2^1S$ and $2^1S \rightarrow 2^1S$ transitions.

E (eV) above 2^1S threshold	$1^1S \rightarrow 2^1S$	$2^3S \rightarrow 2^1S$	$2^1S \rightarrow 2^1S$	E (eV) above 2^1S threshold	$1^1S \rightarrow 2^1S$	$2^3S \rightarrow 2^1S$	$2^1S \rightarrow 2^1S$
0.00734	1.086^{-2}†	1.936	4.080^{3}	1.503	3.439^{-2}	5.203	2.558^{2}
0.0209	1.058^{-2}	4.596	1.166^{3}	1.639	3.563^{-2}	4.822	2.349^{2}
0.0753	1.396^{-2}	1.037^{1}	2.370^{2}	1.912	3.818^{-2}	4.207	1.991^{2}
0.143	1.637^{-2}	1.190^{1}	2.043^{2}	2.183	4.067^{-2}	3.718	1.708^{2}
0.279	2.216^{-2}	1.224^{1}	3.159^{2}	2.455	4.306^{-2}	3.317	1.489^{2}
0.293	2.308^{-2}	1.190^{1}	3.245^{2}	2.727	4.531^{-2}	2.980	1.325^{2}
0.307	2.430^{-2}	1.097^{1}	3.308^{2}	3.000	4.748^{-2}	2.693	1.188^{2}
0.320	2.429^{-2}	8.911	3.182^{2}	3.679	5.214^{-2}	2.134	9.416^{1}
0.334	2.434^{-2}	8.695	3.176^{2}	4.359	5.556^{-2}	1.724	7.827^{1}
0.347	2.449^{-2}	8.681	3.182^{2}	5.719	5.893^{-2}	1.161	5.793^{1}
0.415	2.549^{-2}	9.109	3.282^{2}	5.889	5.909^{-2}	1.107	5.616^{1}
0.551	2.769^{-2}	9.533	3.422^{2}	7.079	5.884^{-2}	7.999^{-1}	4.649^{1}
0.579	2.807^{-2}	9.676	3.449^{2}	8.990	5.515^{-2}	—	3.715^{1}
0.619	2.814^{-2}	9.660	3.483^{2}	9.799	5.300^{-2}	—	3.456^{1}
0.687	2.823^{-2}	9.319	3.512^{2}	6.102^{1}	—	1.106^{-2}	6.541
0.823	2.883^{-2}	8.395	3.480^{2}	7.939^{1}	2.360^{-2}	7.200^{-3}	5.191
0.959	2.972^{-2}	7.526	3.358^{2}	9.939^{1}	1.963^{-2}	4.599^{-3}	4.238
1.095	3.074^{-2}	6.797	3.186^{2}	1.2939^{2}	1.600^{-2}	2.597^{-3}	3.325
1.231	3.186^{-2}	6.160	2.983^{2}	1.7939^{2}	1.230^{-2}	1.226^{-3}	2.447
1.367	3.309^{-2}	5.641	2.768^{2}				

† The superscript denotes the power of ten by which the number should be multiplied.

Other calculations performed are: Born approximation (Moiseiwitsch 1957, Ton-That *et al* 1977, Kennedy 1968, Kim and Inokuti 1969), ten-channel eikonal approximation (Flannery and McCann 1975) and semi-empirical formulae (Johnson 1967, Fujimoto 1978). Among these calculations large discrepancies in magnitude, as well as in shape, exist.

The present calculation for the $2^3S \rightarrow 2^3P$ transition gives cross sections considerably higher than any of the other calculations, except our unitarised Born approximation at intermediate energies (see figure 3), reaching a maximum of about 5 eV above 2^3P threshold. At high energies, the present R-matrix calculations converge to our unitarised Born approximation results.

For the $2^1S \rightarrow 2^1P$ transition (see figure 4), the present calculation is in good agreement with Burke *et al* (1969). At energies greater than 10 eV, the present calculation again is in good accord with the ten-channel eikonal calculation of Flannery and McCann (1975). At high energies, the present R-matrix calculations converge to our unitarised Born results (see figure 3). There are are no experimental measurements of cross section for these transitions. The cross sections for these transitions are also given in tables 3 and 4.

3.2.3. Cross sections for elastic scattering from $2^{3,1}P$ states. The cross sections for elastic scattering from the 2^3P and 2^1P states obtained by the present calculation are given in tables 3 and 4. The present cross sections are larger than those of Oberoi and Nesbet (1973) and Berrington *et al* (1975). It is possible that in the earlier calculations only one parity was considered (see § 3.2.1).

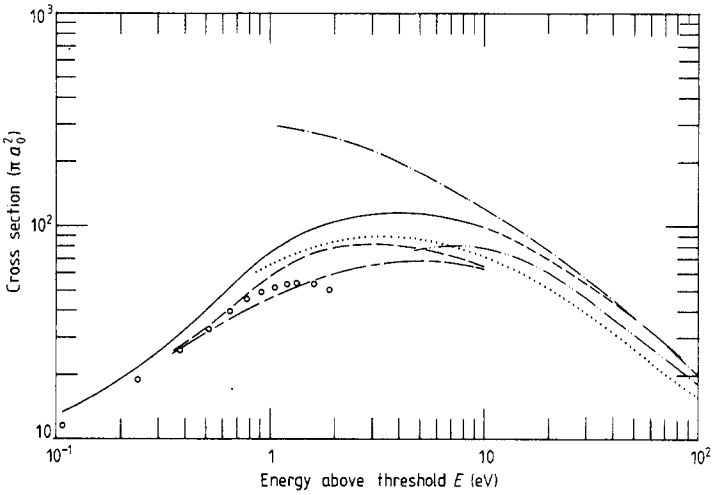

Figure 3. Cross sections (in units of πa_0^2) for the optically allowed transition $2^3S \rightarrow 2^3P$ against electron impact energy (in eV) above 2^3P threshold. Theory: ∘∘∘, R-matrix calculation (Berrington *et al* 1975); ———, present R-matrix calculation; – – –, interpolation of present R-matrix calculation (see § 4); —·—, present unitarised Born calculation; — — —, semi-empirical calculation (Johnson 1967); · · ·, semi-empirical calculation (Fujimoto 1978); — — —, Burke *et al* (1969); — · · —, Flannery and McCann (1975).

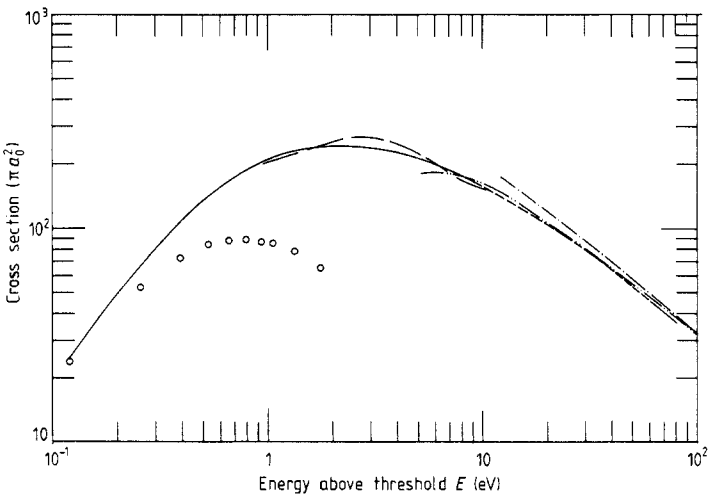

Figure 4. Cross sections (in units of πa_0^2) for the optically allowed transition $2^1S \rightarrow 2^1P$ against electron impact energy (in eV) above 2^1P threshold. Data legend as figure 3.

3.2.4. Cross sections for elastic scattering from 2^3S and 2^1S. The cross sections for elastic scattering from the 2^3S state are given in table 1. In figure 5 our cross sections for total elastic scattering as well as doublet elastic scattering from this state are shown and compared with other calculations. Our completed doublet contributions are in good agreement with those of the close-coupling calculation (Burke *et al* 1969) and those of Oberoi and Nesbet (1973). In accord with the calculation of Oberoi and Nesbet, our

Table 3. Electron excitation cross section (πa_0^2) for the 1^1S–2^3P, 2^3S–2^3P, 2^1S–2^3P and 2^3P–2^3P transitions.

E (eV) above 2^3P threshold	1^1S–2^3P	2^3S–2^3P	2^1S–2^3P	2^3P–2^3P
0.0110	5.797^{-4}†	4.499	2.080^{1}	4.223^{2}
0.0246	1.011^{-3}	6.492	2.711^{1}	4.401^{2}
0.0382	1.433^{-3}	7.989	3.043^{1}	4.886^{2}
0.106	3.415^{-3}	1.344^{1}	3.549^{1}	6.655^{2}
0.242	6.475^{-3}	2.214^{1}	3.483^{1}	4.130^{2}
0.269	7.033^{-3}	2.356^{1}	3.308^{1}	4.037^{2}
0.310	7.522^{-3}	2.594^{1}	3.090^{1}	3.707^{2}
0.378	8.270^{-3}	3.050^{1}	2.843^{1}	3.252^{2}
0.514	9.680^{-3}	4.067^{1}	2.481^{1}	2.740^{2}
0.650	1.106^{-2}	5.104^{1}	2.221^{1}	2.406^{2}
0.786	1.224^{-2}	6.084^{1}	2.024^{1}	2.157^{2}
0.922	1.387^{-2}	6.968^{1}	1.876^{1}	1.962^{2}
1.060	1.531^{-2}	7.724^{1}	1.768^{1}	1.802^{2}
1.194	1.677^{-2}	8.367^{1}	1.694^{1}	1.673^{2}
1.330	1.822^{-2}	8.892^{1}	1.625^{1}	1.563^{2}
1.602	2.111^{-2}	9.694^{1}	1.526^{1}	1.385^{2}
1.874	2.398^{-2}	1.025^{2}	1.433^{1}	1.245^{2}
2.146	2.683^{-2}	1.065^{2}	1.336^{1}	1.130^{2}
2.418	2.968^{-2}	1.096^{2}	1.237^{1}	1.034^{2}
2.690	3.259^{-2}	1.120^{2}	1.140^{1}	9.553^{1}
3.374	4.024^{-2}	1.154^{2}	9.209	7.987^{1}
4.050	4.781^{-2}	1.166^{2}	7.364	6.900^{1}
5.410	6.094^{-2}	1.148^{2}	4.772	5.484^{1}
5.580	6.221^{-2}	1.143^{2}	4.523	5.351^{1}
6.770	6.809^{-2}	1.102^{2}	3.125	4.585^{1}
8.681	6.782^{-2}	1.031^{2}		3.740^{1}
9.490	6.488^{-2}	9.996^{1}		3.470^{1}
6.0711^{1}	—	3.312^{1}		6.786
7.9081^{1}	3.767^{-3}	2.697^{1}		5.321
9.9081^{1}	1.829^{-3}			4.303
1.29081^{2}	8.190^{-4}			3.345
1.79081^{2}	3.100^{-4}			

† The superscript denotes the power of ten by which the number should be multiplied.

curve for the elastic scattering cross sections has peaks corresponding to the ^2P and ^2D shape resonances. There is a sudden increase in the total cross section (doublet + quartet) near the 2^3S threshold. This is produced by a quartet S-wave resonance.

In figure 6 our cross section for elastic scattering from 2^1S is shown and compared with other calculations. The large values of cross sections near the 2^1S threshold are attributed to a 'virtual state' (Burke *et al* 1969, Oberoi and Nesbet 1973). Although our cross section lies slightly higher than that of Oberoi and Nesbet (1973), the present calculation does show similar resonance structure to that observed by them. The peak near the 2^3P threshold is due to the ^2D resonance. This is in good agreement with the calculation of Oberoi and Nesbet (1973).

At low energies, the polarised-core approximation (Husain *et al* 1967) and effective range calculation (Robinson 1969) have also been used to obtain elastic cross sections from 2^3S and 2^1S. These are essentially single-channel approximations. Their results

Table 4. Electron excitation cross section (πa_0^2) for the 1^1S–2^1P, 2^3S–2^1P, 2^1S–2^1P, 2^3P–2^1P and 2^1P–2^1P transitions.

E (eV) above 2^1P threshold	1^1S–2^1P	2^3S–2^1P	2^1S–2^1P	2^3P–2^1P	2^1P–2^1P
0.01224	—	0.315	1.981	3.562	6.617^{2}
0.05304	1.007^{-3}†	0.805	8.898	1.433^{1}	6.104^{2}
0.121	1.809^{-3}	1.336	2.520^{1}	1.394^{1}	5.223^{2}
0.257	3.260^{-3}	1.900	6.612^{1}	1.013^{1}	4.233^{2}
0.393	4.614^{-3}	2.145	1.066^{2}	8.087	3.638^{2}
0.529	5.939^{-3}	2.256	1.411^{2}	6.855	3.208^{2}
0.665	7.295^{-3}	2.305	1.686^{2}	6.092	2.869^{2}
0.801	8.720^{-3}	2.339	1.893^{2}	5.562	2.602^{2}
0.937	1.020^{-2}	2.375	2.060^{2}	5.202	2.386^{2}
1.073	1.172^{-2}	2.398	2.174^{2}	4.948	2.199^{2}
1.345	1.482^{-2}	2.436	2.319^{2}	4.602	1.907^{2}
1.617	1.794^{-2}	2.433	2.386^{2}	4.344	1.680^{2}
1.889	2.104^{-2}	2.386	2.413^{2}	4.110	1.496^{2}
2.161	2.410^{-2}	2.305	2.433^{2}	3.882	1.344^{2}
2.433	2.715^{-2}	2.203	2.434^{2}	3.659	1.222^{2}
3.113	3.483^{-2}	1.911	2.375^{2}	3.124	9.889^{1}
3.793	4.256^{-2}	1.627	2.292^{2}	2.635	8.343^{1}
5.153	5.758^{-2}	1.150	2.116^{2}	1.839	6.458^{1}
5.323	5.936^{-2}	1.100	2.093^{2}	1.758	6.287^{1}
6.513	7.102^{-2}	8.090^{-1}	1.930^{2}	1.286	5.318^{1}
8.424	8.649^{-2}	4.987^{-1}	1.731^{2}	7.953^{-1}	4.287^{1}
9.233	9.196^{-2}	4.102^{-1}	1.654^{2}	6.543^{-1}	3.954^{1}
6.0454^{1}	1.604^{-1}		4.483^{1}	1.560^{-2}	7.452
7.8823^{1}	1.491^{-1}		3.558^{1}	9.378^{-3}	5.846
9.8824^{1}	1.389^{-1}			5.709^{-3}	4.729
1.28824^{2}	1.258^{-1}				3.682
1.78824^{2}	1.090^{-1}				

† The superscript denotes the power of ten by which the number should be multiplied.

tend to lie substantially higher than the present calculations and the resonance structure is not correctly brought out in their calculations. Marriott (1966) had also carried out close-coupling calculations for these transitions. His results lie considerably lower than the present calculations (see figures 5 and 6) and again no resonance is observed. This may be due to the fact that the $2^{1,3}P$ states are not coupled with any of the $2^{1,3}S$ states in his calculation and hence polarisation of the atom is not fully treated. Due to the narrow energy spacing between the $2^{1,3}S$ and $2^{1,3}P$ states, the 2^3S–2^3P and 2^1S–2^1P couplings which are included in our formalism, account for nearly all the dipole polarisation for the 2^3S and 2^1S states. The calculations of the adiabatic-exchange approximation and the extended-polarisation approximation (Sklarew and Callaway 1968) are not consistent in the treatment for elastic scattering from the 2^3S and 2^1S states. The resonance structure is not brought out in these calculations. In contrast to the small dipole polarisability from ground-state helium (1.4 a_0^3), the metastable $2^{1,3}S$ state of helium has high dipole polarisabilities (316 a_0^3 for 2^3S and 802 a_0^3 for 2^1S, Chung and Hurst 1966) which slows the convergence of the cross sections for the $2^{1,3}S \rightarrow 2^{1,3}S$ transitions. Again the polarised-orbital calculations are in a single-channel scattering approximation which does not allow for any loss of flux to the other open channels.

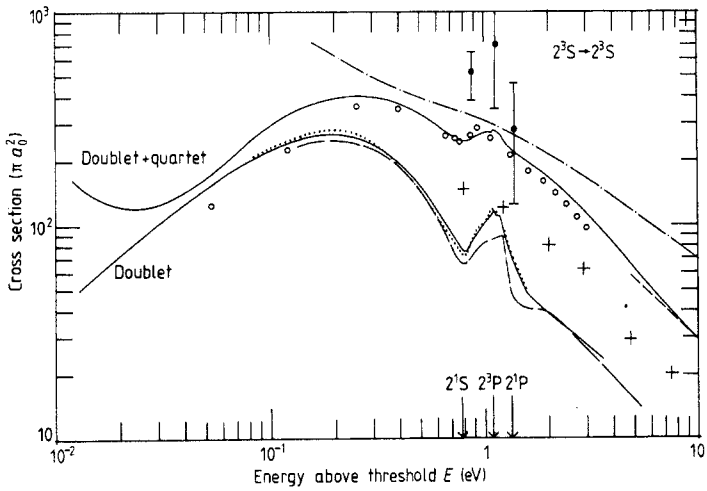

Figure 5. Elastic cross sections (in units of πa_0^2) from 2^3S state against electron impact energy (in eV) above 2^3S threshold. Data as for figure 1 with: ●, experimental measurements of Neynaber *et al* (1964) for total cross sections from 2^3S state; — · —, calculation of Robinson (1969); +, close-coupling calculation of Marriott (1966); ——, Burke *et al* (1969); – – –, first Born approximation Taylor 1975).

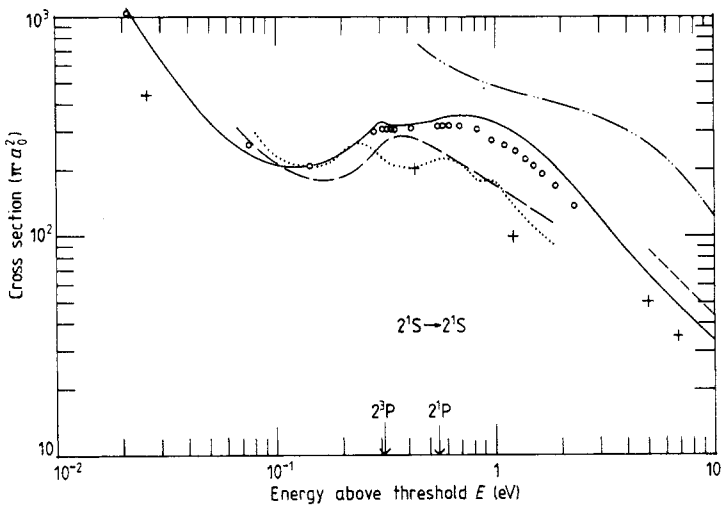

Figure 6. Elastic cross sections (πa_0^2) from 2^1S state against electron impact energy (eV) above 2^1S threshold. Data as for figure 5 with: —· · —, calculation of Husain *et al* (1967).

At high energies, the first Born (Taylor 1975) and Glauber calculations (Chen and Khayrallah 1976) are available for the elastic cross sections from the 2^3S and 2^1S states. The present calculations seem to converge to the first Born calculation of Taylor (1975) at high energies. The convergence of our R-matrix results to our unitarised Born results at high energies is very slow, for example in the case of elastic scattering of 2^3S our R-matrix results are greater than the Born results by 28% and 24% at 10 and 100 eV respectively.

3.2.5. Total cross sections for electrons scattered from 2^3S and 2^1S states of helium. In contrast to collisions involving ground-state helium atoms relatively little is known about transitions between excited states of helium. Only two experimental measurements (Neynaber *et al* 1964, Wilson and Williams 1976) have been performed to determine the total cross sections for low-energy electrons on He($2^{1,3}$S). When these measurements were compared with the theoretical elastic scattering cross sections, it was found that above approximately 1 eV the measurements were much larger than the theoretical elastic scattering cross sections. The theoretical elastic cross sections decreased rapidly with energy while the measured cross section decreased very slowly with energy. In order to explore this discrepancy we have also calculated the de-excitation cross sections for $2^1S \rightarrow 2^3S$, $2^1S \rightarrow 1^1S$ and $2^3S \rightarrow 1^1S$ (shown in figure 7 except

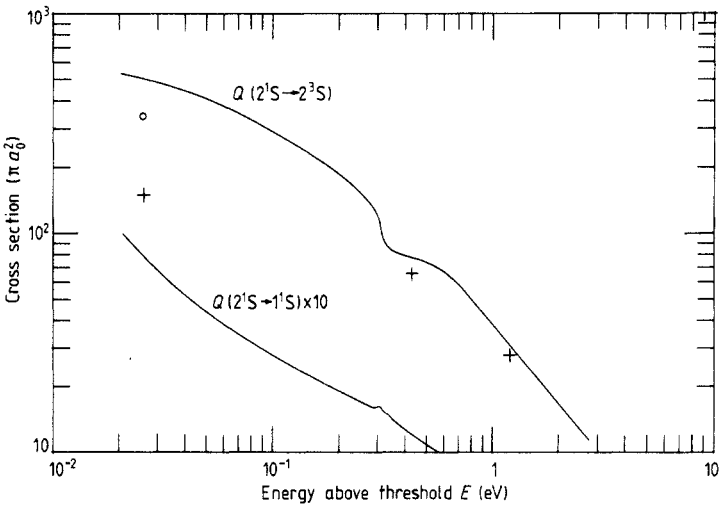

Figure 7. $2^1S \rightarrow 2^3S$ and $2^1S \rightarrow 1^1S$ de-excitation cross sections (πa_0^2) against electron impact energy (eV) above 2^1S threshold. Theory: ———, present R-matrix calculation; +, Marriott's calculation for $2^1S \rightarrow 2^3S$ de-excitation cross section. Experiment: ○, Phelps (1955) measurement for $2^1S \rightarrow 2^3S$ de-excitation cross section.

$2^3S \rightarrow 1^1S$). It was found that contributions from $2^1S \rightarrow 2^3S$ and $2^1S \rightarrow 1^1S$ are important only for very low incident electron energies, and the $2^3S \rightarrow 1^1S$ contribution is insignificant (when compared with the elastic cross section $2^3S \rightarrow 2^3S$) and therefore cannot resolve the discrepancy with the experimental data at $E \geqslant 1$ eV. However, if we were to add the contributions from the optically allowed transitions $2^1S \rightarrow 2^1P$ and $2^3S \rightarrow 2^3P$ to that of the de-excitation and elastic cross sections from the $2^{1,3}$S state, there is good agreement between the present calculation and the measurements of Neynaber *et al* (1964) and Wilson and Williams (1976) (see figure 8). The optically allowed transitions are very strong transitions and become increasingly dominant for impact energies above 1 eV (above $2^{1,3}$S thresholds). The present calculation on total cross sections from the $2^{1,3}$S state has not included the contributions from transitions to $n \geqslant 3$ states (which are not expected to be important). However, the contribution from ionisation from the $2^{1,3}$S state may be significant and it would further enhance the

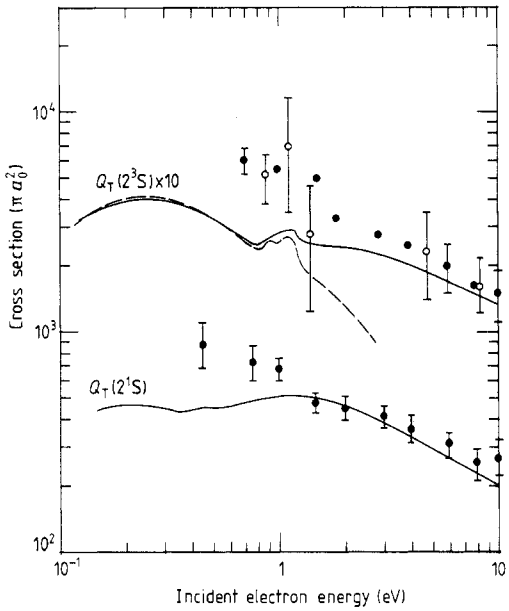

Figure 8. Total cross sections (πa_0^2) from 2^3S and 2^1S state against electron impact energy (eV) above 2^3S and 2^1S thresholds respectively. Theory: ———, present *R*-matrix calculation; — — —, Oberoi and Nesbet (1973). Experiment: ○, Neynaber *et al* (1964); ●, Wilson and Williams (1976).

agreement between the present calculations and the experiments. The dominance of the transitions $2^3S \rightarrow 2^3P$ and $2^1S \rightarrow 2^1P$ over other transitions from $2^{1,3}S$ states at energies greater than 1 eV suggests that as the incident electron energy exceeds the $2^{1,3}P$ thresholds, the loss of flux to the $2^1S \rightarrow 2^1P$ and $2^3S \rightarrow 2^3P$ channels is very substantial and hence calculations based on a single-channel scattering approximation may not be expected to be good.

4. Intermediate- and high-energy cross sections

For optically allowed transitions the electron excitation cross section at large energies may be written as

$$Q(\pi a_0^2) = \frac{A \lg E}{E} + \frac{B}{E} + \frac{C}{E^2} + \frac{D}{E^3} + \frac{F}{E^4} + \frac{G}{E^5} \tag{2}$$

where E is the energy of the electron in eV above the excitation threshold. If a transition is not optically allowed $A = 0$ and if a transition is spin forbidden $B = 0$ and $C = 0$. In order to allow our results to be extended into the energy range where pseudo-resonances are important we have fitted our cross sections above and below the pseudo-resonance region to (2).

The results are given in table 5. The accuracy of the fits over the energy range in which they are fitted is also indicated in table 5. For elastic scattering, optically allowed and spin-allowed transitions these fits can be used to extrapolate the results to high energies. However, for spin-forbidden transitions the fits should only be used in the

Table 5. Coefficients in the expansion (2) of the electron excitation cross section.

Transition	A	B	C	D	F	G	Range (eV) above threshold	Accuracy (%)
1^1S–2^3S	0.0	0.0	1.4325^1	-1.3838^2	4.2052^2	0.0	7–180	20
1^1S–2^1S	0.0	2.3031	-3.1168^1	1.3413^2	0.0	0.0	7–∞	7
1^1S–2^3P	0.0	0.0	0.0	2.1330^3	-3.6718^4	1.6136^5	9–180	10
1^1S–2^1P	2.3017^1	-3.3608^1	1.4433^2	-2.8928^2	0.0	0.0	6.5–∞	3
2^3S–2^3S	0.0	3.8336^2	-1.7831^3	8.1625^3	0.0	0.0	6.5–∞	2
2^3S–2^1S	0.0	0.0	4.3449^1	5.5562	-2.0819^2	0.0	3.0–180	10
2^3S–2^3P	9.1407^2	4.6801^2	-5.5561^3	1.5561^4	0.0	0.0	5.5–∞	3
2^3S–2^1P	0.0	0.0	4.6156^1	-6.4272^1	-8.3453^1	0.0	3–9	10
2^1S–2^1S	0.0	4.3515^2	-1.4437^3	4.8804^3	0.0	0.0	5–∞	5
2^1S–2^3P	0.0	0.0	1.8382^2	-1.9920^2	-2.2717^2	0.0	2.7–6.8	5
2^1S–2^1P	1.0025^3	1.0088^3	-5.2837^3	1.0481^4	0.0	0.0	5–∞	1
2^3P–2^3P	0.0	4.3870^2	-1.3961^3	3.3961^3	0.0	0.0	5–∞	5
2^3P–2^1P	0.0	0.0	5.6720^1	2.2947^1	-3.2776^2	0.0	5–99	5
2^1P–2^1P	0.0	4.8194^2	-1.4808^3	3.7092^3	0.0	0.0	5–∞	2

energy range given in table 5, as in this energy range our results can usually be fitted best by taking $C \neq 0$ whereas we would expect $C = 0$ at very high energies.

5. Conclusion

We have presented five-state R-matrix calculations for the integrated cross sections for transitions between the five lowest states (1^1S, 2^3S, 2^1S, 2^3P, 2^1P) of helium over the energy range from the first excitation threshold to approximately 200 eV. At low energies, the calculations of Berrington *et al* (1975) have been revised. At higher energies, five-state unitarised Born approximations were used to provide higher partial waves to ensure convergence on cross sections. Sufficient energy points were obtained to establish the shape of the cross section as a function of incident energy. Comparison with other theoretical calculations and experimental measurements was made whenever possible. There was good agreement between the present calculations on cross sections with available experimental measurements. There is a paucity of experimental data and theoretical calculations for scattering from the $n = 2$ states. The present calculation represented the first serious attempt to provide an *ab initio* estimate on such data.

Acknowledgments

We wish to thank Professor M R Flannery for sending us tabulated values of his cross sections and Professor T Fujimoto for sending us his preprint before publication. Stimulating discussion with Dr J A Tully is also gratefully acknowledged.

One of us (WCF) would like to acknowledge his gratitude to the Association of Commonwealth Universities for an Academic Staff Fellowship. The calculations were carried out using a link to the IBM 370/165 at the Daresbury Laboratory provided by a grant from the Science Research Council.

References

Berrington K A, Burke P G and Sinfailam A L 1975 *J. Phys. B: At. Mol. Phys.* **8** 1459–73
Bhattacharyya T 1961 *Ind. J. Phys.* **35** 623–7
Burke P G, Cooper J W and Ormonde S 1969 *Phys. Rev.* **183** 245–64
Chen S T and Khayrallah G A 1976 *Phys. Rev.* A **14** 1639
Chung K T and Hurst R P 1966 *Phys. Rev.* **152** 35
Flannery M R and McCann K J 1975 *Phys. Rev.* A **12** 846–55
Flannery M R, Morrison W R and Richmond B L 1975 *J. Appl. Phys.* **46** 1186–90
Fon W C, Berrington K A, Burke P G and Kingston A E 1979 *J. Phys. B: At. Mol. Phys.* **11** 1861–72
Fon W C, Berrington K A and Hibbert A 1981 *J. Phys. B: At. Mol. Phys.* **14** 307–21
Fon W C, Berrington K A and Kingston A E 1980 *J. Phys. B: At. Mol. Phys.* **13** 2309–25
Fujimoto T 1978 *Report* IPPJ-AM-8 Nagoya University (Japan)
Husain D, Choudhury A L, Rafiqullah A K, Nestor C W Jr and Malik F B 1967 *Phys. Rev.* **161** 68–73
Johnson L C 1967 *Phys. Rev.* **155** 64
Kennedy D J 1968 *PhD Thesis* The Queen's University of Belfast
Kim Y K and Inokuti M 1969 *Phys. Rev.* **181** 205–13
Marriott R 1966 *Proc. Phys. Soc.* **87** 407–15
Moiseiwitsch B L 1957 *Mon. Not. R. Astron. Soc.* **117** 189–92
Neynaber R H, Trujillo S M, Marino L L and Rothe E W 1964 *Atomic Collision Processes* ed M R C McDowell (Amsterdam: North-Holland)
Oberoi R S and Nesbet R K 1973 *Phys. Rev.* A **8** 2969–79
O'Malley T F, Burke P G and Berrington K A 1979 *J. Phys. B: At. Mol. Phys.* **12** 953–65
Phelps A V 1955 *Phys. Rev.* **99** 1307–13
Robinson E J 1969 *Phys. Rev.* **182** 196–200
Rosenberg L, O'Malley T F and Spruch L 1961 *J. Math. Phys.* **2** 491–8
Sklarew R C and Callaway J 1968 *Phys. Rev.* **175** 103–12
Taylor I R 1975 *J. Phys. B: At. Mol. Phys.* **8** 2810–6
Ton-That D, Manson S T and Flannery M R 1977 *J. Phys. B: At. Mol. Phys.* **10** 621–35
Tully J A and Summers H P 1979 *Astrophys. J.* **229** L113–4
Wilson W G and Williams W L 1976 *J. Phys. B: At. Mol. Phys.* **9** 423–32